



Repositorio Institucional de la Universidad Autónoma de Madrid

<https://repositorio.uam.es>

Esta es la **versión de autor** del artículo publicado en:

This is an **author produced version** of a paper published in:

The Journal of Physical Chemistry C, 122.26 (2018): 14838–14845

DOI: <http://dx.doi.org/10.1021/acs.jpcc.8b03937>

Copyright: © 2018 American Chemical Society

El acceso a la versión del editor puede requerir la suscripción del recurso
Access to the published version may require subscription

Effect of H₂O and D₂O Thermal Anomalies on the Luminescence of Eu³⁺ Aqueous Complexes

Lucía Labrador-Páez^{1,2}, Eduardo Montes^{1,3}, Marco Pedroni¹, Patricia Haro-González^{1,2}, Marco Bettinelli⁴, Daniel Jaque^{1,2,5}, José García-Solé^{1,2,*} and Francisco Jaque¹

¹*Fluorescence Imaging Group, Departamento de Física de Materiales, Universidad Autónoma de Madrid, 28049, Madrid, Spain*

²*Instituto Universitario de Ciencia de Materiales Nicolás Cabrera, Universidad Autónoma de Madrid, 28049, Madrid, Spain*

³*Grupo de Espectroscopia de Materiales Avanzados y Nanoestructurados, GEMANA, Centro de Investigaciones en Óptica A.C., 37150 León, Guanajuato, México*

⁴*Luminescence Materials Laboratory, Dipartimento di Biotecnologie, Università di Verona, 37134, Verona, Italy*

⁵*Instituto Ramón y Cajal de Investigación Sanitaria (IRYCIS), 28034, Madrid, Spain*

*E-mail: jose.garcia_sole@uam.es

Abstract

Aqueous solutions of luminescent metal-ion complexes, in particular those of lanthanide ions, can play an essential role in biomedical applications. For all these applications, the knowledge about the influence of temperature variations within the physiological range (20-60 °C) on their optical properties becomes essential. At variance with other liquids, water is unique as it does present an anomalous temperature dependent behavior. In particular, most of water properties present remarkable physico-chemical changes above a certain temperature, which ranges between 30 and 50 °C. In this work we systematically investigate the effect of temperature on the luminescence properties of Eu³⁺ ions when dissolved either in H₂O or D₂O. An anomalous thermal behavior, manifested as a bilinear trend, with crossover at around 35 °C for H₂O and 38 °C for D₂O, is found in a variety of Eu³⁺ optical spectroscopic properties (branching ratio, luminescence lifetime, and emission band shape). The observed changes are here tentatively explained in terms of a different aggregation state of H₂O and D₂O molecules below and above crossover temperature. Such changes in the molecular clustering lead to a temperature induced change in the relative concentrations of the 8-fold and 9-fold coordinated Eu³⁺ complexes. Finally, we have observed that the pH of the aqueous solution plays an essential role in defining the temperature at which the anomaly takes place, so that the differences in the values reported in the literature for the crossover temperature are accounted for.

Introduction

Liquid water is the essential dispersion medium for luminescent compounds and materials with potential bio-applications, such as biomolecules, nanoparticles, and coordination compounds.¹⁻³ In general, water has been considered as a simple solvent showing the regular properties of any fluid in the physiological temperature range (20-60°C). However, this assessment is far from being a correct description. Indeed, water is a quite complex fluid that displays unusual properties, such as a density maximum at about 4 °C, which is still a matter of debate.⁴⁻⁵ In addition, an anomaly in the dielectric constant of liquid water at about 50 °C (within the physiological temperature range) has been recently discovered.⁶ This anomaly was evidenced as a bilinear behavior in the temperature dependence of the dielectric constant (typically fluids show a linear temperature dependence), with the two linear trends crossing at about 50 °C, this being denoted as the “crossover temperature” (hereafter T_{cross}).⁶⁻⁷ Subsequent studies have established that this crossover behavior has its own signature on a variety of physico-chemical properties of liquid water such as thermal conductivity, proton spin-lattice relaxation time, refractive index, surface tension, piezo-optical coefficient, acidity, heat capacity, and isothermal compressibility.⁸⁻¹¹ The dielectric response of water for temperatures below T_{cross} has been tentatively explained by considering the presence of small water molecular clusters with an electric dipole moment (μ) close to that of the ice phase ($\mu_{\text{ice}} = 2.18$ D). However, for temperatures above T_{cross} , the dielectric response is better explained as due to individual water molecules with an electric dipole moment close to that of the vapor phase ($\mu_{\text{vapor}} = 1.87$ D).^{7-8, 12} This anomalous de-clustering affects not only intrinsic water properties, but also properties of the solutes and nanoparticles dispersed in it. Indeed, the impact of this crossover on the aqueous dispersion of optically active nanoparticles has been already reported. It does affect the interactions between colloidal lanthanide-doped dielectric nanoparticles, the plasmon resonance of metal nanoparticles, and the spectroscopic properties of small quantum dots.^{7-9, 13} Based on all these evidences, it is reasonable to expect that this water structural crossover would also influence the temperature dependence of the luminescent properties of complexes in aqueous environments.¹⁴⁻¹⁶ Nevertheless, despite its great interest from both fundamental and applied points of view, such influence has not been reported so far, to the best of our knowledge.

When investigating the possible influence of water structural crossover on the spectroscopic properties of luminescent complexes, it is critical to select a highly sensitive luminescent entity. In this sense, Eu^{3+} ion-based complexes seem to be especially suitable. Indeed, the Eu^{3+} luminescence has proved its suitability for evidencing small changes in the local environment of this ion.¹⁷⁻¹⁸ Eu^{3+} shows several emission bands in the visible range as a result of radiative de-excitation from the $^5\text{D}_0$ excited state to various $^7\text{F}_J$ lower energy states (from $J = 0$ to 4).¹⁹⁻²⁰ In particular, the $^5\text{D}_0 \rightarrow ^7\text{F}_2$ transition has a forced electric dipole (ED) nature and so its intensity is hypersensitive to local environmental changes.²¹⁻²² In addition, according to the first order perturbation treatment of the Judd-Ofelt theory, the ED $^5\text{D}_0 \rightarrow ^7\text{F}_0$ transition is strictly forbidden. However, in some cases, it is weakly observed as a result of

J-mixing, i.e. due to wave functions admixing of the involved states (5D_0 and 7F_0) with other $J \neq 0$ states (5D_2 and 7F_2) caused by the presence of even parity terms in the crystal field.²¹⁻²² In these cases, this singlet-to-singlet transition ($J=0$ in both involved energy levels) is very convenient as any asymmetry in the band shape clearly indicates the presence of different local environments, i.e. non-equivalent Eu^{3+} species. Finally, the $^5D_0 \rightarrow ^7F_1$ emission is of singular importance as can also be used to calibrate the full Eu^{3+} emission spectrum originating from the 5D_0 excited state. This transition is of magnetic dipole (MD) character and so its intensity is largely independent of the local environment of Eu^{3+} ions.²³ All these features make Eu^{3+} complexes excellent candidates to investigate the water structural crossover in the physiological temperature range.

Under this scenario, we have systematically investigated the temperature dependence of the emission of Eu^{3+} aqueous complexes in both H_2O and D_2O as a new strategy to get further understanding on the physical-chemical phenomena behind the water structural crossover. The reason for considering also deuterated water solutions is double: (i) O-H vibrations strongly quench the Eu^{3+} emission spectrum, while O-D vibrations do not; and (ii) experimental evidence also exists of a structural crossover in D_2O .^{13, 24} We here show how certain luminescent features of Eu^{3+} ions (branching ratios and radiative and non-radiative transition rates) are affected by the water structural crossover. In addition, the $^5D_0 \rightarrow ^7F_0$ emission band, which is sensitive to the presence of different environments (i.e. aqueous complexes with different number of water molecules in the first coordination sphere)²⁵, and so it is influenced by the relative concentration of the two main coordination complexes $[\text{Eu}(\text{H}_2\text{O})_8]^{3+}$ and $[\text{Eu}(\text{H}_2\text{O})_9]^{3+}$.

Methods

$\text{EuCl}_3 \cdot 6\text{H}_2\text{O}$ (99.99%) was purchased from Sigma-Aldrich, whilst D_2O (99.9%) was purchased from Euriso-Top solvents. Both these reagents were used as received without further purification. The starting solutions (0.1 M) were prepared by dissolving 73 mg of $\text{EuCl}_3 \cdot 6\text{H}_2\text{O}$ (0.2 mmol) in 2 ml of deionized water (milliQ) or of deuterium oxide. The concentration used in the experiments is the smallest for which the luminescence signal is detectable by our experimental set-up. It is reasonable to assume that the Cl^- ion, which is weakly coordinating in water to lanthanide ions, does not bind to Eu^{3+} , i.e. that only aqueous complexes of Eu^{3+} ions are present.²⁶ The pH value at 20 °C for the Eu^{3+} solution in H_2O was 5.5.

Luminescence experiments were carried out by using a 405 nm laser diode as excitation source. The excitation beam was focused into the sample by an objective lens, which also collects the luminescence. The emission was discriminated from excitation by means of a wavelength selective mirror. Then it was spectrally analyzed by a monochromator (iHR320, Horiba) and recorded by a cooled CCD array detector (Synapse, Horiba). For temperature dependent experiments, the solutions were placed in 200 μm height chamber (Ibidi Inc., $\mu\text{-}$

Slide I Leuer 80161). The chamber was placed on a controlled temperature stage. Then the temperature was varied from 10 up to 70 °C with a resolution of 0.1 °C. The solutions were maintained for 10 minutes at each particular temperature, so that they were considered to be at thermal equilibrium. The same results were obtained from heating and cooling processes.

Intensity decay measurements were carried out upon pulsed laser excitation by an optical parametric oscillator at 521 nm, i.e. under excitation of the 5D_1 energy level. The emitted luminescence was analyzed by a monochromator after passing through appropriate filters. The intensity decay of the transition $^5D_0 \rightarrow ^7F_1$ of Eu^{3+} , i.e. the decay curve from the 5D_0 state, was acquired by using a photomultiplier tube (Hamamatsu, R928) and a digital oscilloscope.

Results & discussion

Figure 1 shows representative emission spectra corresponding to the Eu^{3+} aqueous complexes in D_2O and H_2O solutions at different temperatures, obtained upon laser excitation at 405 nm ($^7F_0 \rightarrow ^5L_6$ transition of Eu^{3+} (see inset in Figure 1)). The different emission bands can be easily assigned to specific transitions from the excited state 5D_0 to different 7F_J terminal states of the Eu^{3+} ion.^{25, 27} As mentioned above, the $^5D_0 \rightarrow ^7F_1$ transition is of MD character and, therefore, insensitive to the Eu^{3+} environment. Thus, all the emission spectra were normalized to this transition. The analysis of the normalized emission spectra reveals significant temperature-induced changes in the relative intensities (branching ratios) of the different $^5D_0 \rightarrow ^7F_J$ bands (especially for $J=2$ and 4), which unequivocally indicates that temperature variation induces small changes in the local environments of Eu^{3+} ions.^{19, 23} To account for this temperature-induced environmental effect, it results particularly suitable to study the intensity ratio I_{tot}/I_{MD} , where I_{tot} is the total integrated emission intensity generated from the 5D_0 state and I_{MD} is the integrated intensity of the $^5D_0 \rightarrow ^7F_1$ emission band, which is of MD nature. **Figure 2** displays the I_{tot}/I_{MD} ratio of Eu^{3+} emission as a function of temperature for both H_2O and D_2O solutions. In both cases, a bilinear increasing behavior is observed, with a T_{cross} of about 35°C for H_2O and 38°C for D_2O .

In order to elucidate the origin of these spectroscopic changes, we have investigated the temperature dependence of the Eu^{3+} emission decay time of the 5D_0 energy level. **Figure 3(a)** shows the decay curves obtained from both H_2O and D_2O solutions at room temperature. In both cases, exponential decays are observed with decay constants of 0.114 ± 0.002 ms for H_2O and 2.81 ± 0.02 ms for D_2O . As previously reported, the strong decrease in the lifetime observed for the H_2O solution is due to efficient vibrational relaxation from the 5D_0 excited state of Eu^{3+} , due to the O-H high energy vibrations of the coordinated water molecules.²⁸⁻²⁹ The replacement of H_2O by D_2O strongly suppresses this quenching, as the O-D groups have a much lower stretching wavenumber (2500 cm^{-1} compared to 3400 cm^{-1} , implying about 5 and 3.5 vibrational quanta, respectively, to bridge the energy gap to the lower electronic state).³⁰ **Figure 3(b)** and **3(c)** show the temperature dependence of the 5D_0 lifetime for both

Eu³⁺ solutions. In both cases, the lifetime decreases with temperature. In addition, bilinear trends are observed with T_{cross} similar to those found for the temperature dependence of $I_{\text{tot}}/I_{\text{MD}}$ (Figure 2).

From the experimental data given in Figure 2 and 3 it is possible to estimate the radiative, A_{rad} , and non-radiative, A_{nrad} , transition rates from the ⁵D₀ state as a function of temperature. Werts *et al.*²³ have demonstrated that the radiative lifetime of the ⁵D₀ state, τ_{rad} , can be properly calculated from the ⁵D₀ → ⁷F_J corrected emission spectrum by:

$$\frac{1}{\tau_{\text{rad}}} = A_{\text{MD}} n^3 \frac{I_{\text{tot}}}{I_{\text{MD}}} \quad (1)$$

where n is the refractive index of the solvent and A_{MD} is the spontaneous emission probability for the ⁵D₀ → ⁷F₁ transition *in vacuo*. This value has been theoretically calculated to give $A_{\text{MD}} = 14.65 \text{ s}^{-1}$.³¹ Consequently, using Equation (1) and the obtained temperature trends for $I_{\text{tot}}/I_{\text{MD}}$ (see Figure 2), we can estimate the temperature dependence of τ_{rad} , included in Figure 2. A decrease of τ_{rad} with temperature is observed from a value of 9.89 ms for D₂O (9.64 ms for H₂O) at 10°C to a value of 9.44 ms (9.30 ms for H₂O) at 70°C. The crossover is also evidenced in τ_{rad} for both solutions as a bilinear behavior that reveals a critical temperature close to 35 °C for H₂O and 38 °C for D₂O.

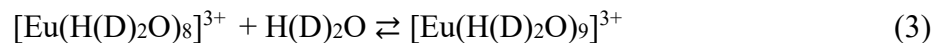
In order to get physical insight into the temperature dependence of τ_{rad} , in the following we focus our attention to the data obtained from the D₂O solution, where the signature of the structural crossover is more evident. **Figure 4(a)** shows the evolution of A_{rad} with temperature (estimated by means of equation (1), $A_{\text{rad}} = 1/\tau_{\text{rad}}$, and from the data in Figure 2). The increase in A_{rad} strongly suggests that a more asymmetric environment occurs as temperature is raised. Such asymmetry leads to a larger admixing of the 4f⁶ wavefunctions with higher energy electronic configurations of different parity and so increasing the radiative rate via electric dipole forced transitions.²⁰ The bilinear behavior is again a clear indication of two different local environments predominating below and above T_{cross} . The non-radiative rate A_{nrad} can be also obtained at each temperature just by considering that:

$$A_T = A_{\text{rad}} + A_{\text{nrad}} \quad (2)$$

where A_T is the total depopulation rate ($A_T = 1/\tau_{\text{tot}}$, τ_{tot} being the experimental ⁵D₀ lifetime included in Figure 3(c)). Both estimated temperature dependences of A_{nrad} and A_T are included in Figures 4(b) and 4(c). A careful comparison between data included in Figure 4(b) and 4(c) indicates that the major contribution to the variation of lifetime with temperature is due to A_{nrad} , i.e. to non-radiative relaxation. At this point, it is important to mention that while the thermal quenching of Eu³⁺ in H₂O is clearly dominated by multi-phonon relaxation due to the O-H vibrations, for Eu³⁺ in D₂O the non-radiative relaxation via O-D vibrations is not high enough to quench the Eu³⁺ emission, due to the high vibrational O-D frequency (~ 2000

cm⁻¹). As a result, it is reasonable to assume the possibility of some amount of quenching via charge transfer state, as reported to occur in different organic matrices.³² Indeed, spectral evidence of charge transfer in Eu³⁺ aqueous solutions was given by Jorgensen *et al.* in 1963.³³ Although this aspect must be corroborated, it could qualitatively explain the different slopes in the temperature dependences observed for the luminescence lifetime for H₂O (Figure 3b) and D₂O (Figure 3c).

Up to now, experimental data included in Figure 2, 3, and 4 reveal that the water structural crossover has a clear signature on the thermal quenching of Eu³⁺ aqueous complexes, but they do not provide any information about the physical-chemical effects behind this phenomenon. In order to correlate the water structural changes and the variations in Eu³⁺ emission properties, we now analyze the temperature dependence of the ⁵D₀ → ⁷F₀ emission band. As expounded above, this singlet emission is influenced by the existence of non-equivalent local environments. **Figure 5** shows the temperature dependence of the ⁵D₀ → ⁷F₀ emission peak. It is observed that this emission experiences a blue shift as the temperature is raised. In addition, a remarkable change in the magnitude of this linear shift is observed at T_{cross}, so that the slope is larger above T_{cross}. Temperature induced ⁵D₀ → ⁷F₀ blue shift has been reported to occur for different Eu³⁺ ion doped host crystals as a result of electron-phonon coupling.³⁴⁻³⁵ Thus, in a similar way, we can state that the blue shift here observed is due to electron-vibration coupling in the Eu³⁺ complex of solution in D₂O. Indeed, in the short temperature range here investigated, the observed linear trends seem to be reasonable.³⁴ However, to account for the bilinear behavior, additional features should be considered. The inset in **Figure 5** shows the ⁵D₀ → ⁷F₀ emission at two different temperatures: one well below T_{cross} (10°C) and one well above T_{cross} (60°C). The spectrum at 10 °C peaks at 17273.5 cm⁻¹ and it has a full width at half maximum of 12 cm⁻¹. It displays a Lorentzian shape that resembles that simulated by means of molecular dynamics and related to [Eu(H₂O)₈]³⁺ complexes.²⁵ Nevertheless, it is generally accepted that Eu³⁺ ions form two different aqueous complexes, one with 8-fold coordination, [Eu(H₂O)₈]³⁺, and other one with 9-fold coordination, [Eu(H₂O)₉]³⁺. In fact, by means of refined analysis of the molecular dynamics trajectories, Clavaguéra *et al.*³⁶ predicted that Eu³⁺ ions are prevalingly 8-fold coordinated (about 63%) at room temperature, but a certain fraction (37%) is in 9-fold coordination. Therefore, it is reasonable to assume that, at each temperature, there are two possible Eu³⁺ environments, according to an equilibrium given by:



As a result, the observed ⁵D₀ → ⁷F₀ emission should be a convolution of two emission bands due to non-equivalent Eu³⁺ sites. We now state that the dominant coordination below T_{cross} is 8 and so its emission shape must be mostly due to this coordination.^{25, 27, 36-38} As the temperature is raised, the corresponding peak position shifts towards blue with a constant slope up to T_{cross}. However, above T_{cross} the peak position blue shifts with a larger slope. In

addition, the spectrum becomes comparatively broader and more asymmetric (see the spectrum at 60 °C in the inset in Figure 5) than those obtained below T_{cross} . It seems that a new component of higher energy grows, accounting for the observed broadening and the increasing asymmetry of the ${}^5\text{D}_0 \rightarrow {}^7\text{F}_0$ emission profile at temperatures above T_{cross} . Thus, the increase in shape asymmetry as well as part of the blue shift observed for the emission above T_{cross} , could be explained as a result of an increase of the concentration of 9-fold coordinated Eu^{3+} ions with respect to the 8-fold ones. Consequently, the main effect of the crossover would be to produce a relative increase in the concentration of the Eu^{3+} complexes with coordination 9, with emission at higher energy, with respect to the Eu^{3+} complexes with coordination 8. For the 8-fold coordinated complex, molecular dynamics simulations have suggested that the 8 coordinating water molecules are arranged to form a square antiprism around Eu^{3+} ions, these ions facing O atoms of the surrounding water molecules (see Figure 6).³⁷ For the 9-fold coordinated complex, the structure has not been assigned to any well-known local structure, and so it is speculative (see Figure 6).³⁹ Nevertheless, the smaller coordination number (8) is responsible for smaller Eu-O distances, presumably leading to increased overlap of the electronic clouds of the two ions and to partial localization of the europium electrons on the oxygen ligands. Due to this nephelauxetic effect, a shift towards lower energy in the ${}^5\text{D}_0 \rightarrow {}^7\text{F}_0$ emission peak is expected in comparison to the aqueous complex with higher coordination number, this being in accordance with the asymmetric broadening at the high energy side of the ${}^5\text{D}_0 \rightarrow {}^7\text{F}_0$ emission band observed over T_{cross} (see inset in Figure 5).^{22, 40-41}

Furthermore, the pronounced change in the relative concentration of the Eu-aqueous complexes that we propose to occur above T_{cross} , can be tentatively explained by considering how water molecules interact below and above T_{cross} . It has been proposed that water molecules are arranged as small clusters for temperatures below T_{cross} , whilst above T_{cross} water properties can be better described by considering weakly interacting water molecules.^{7-8, 12-13} The increase in concentration of these “free” water molecules above T_{cross} would shift the hydration equilibrium of the Eu^{3+} species (Equation (3)) to the right hand side and increases the concentration of $[\text{Eu}(\text{H}_2\text{O})_9]^{3+}$ complexes, as we have schematically displayed in Figure 6. This would explain the changes that we have observed in both temperature induced blue shift and in band shape above T_{cross} (see again Figure 5).

Moreover, the temperature effect on the relative concentrations of the two hydrated coordination compounds can account for the crossover effect on the de-excitation rates, and so it could explain the experimental results given in Figures 2 and 3. Both A_{rad} and A_{nrad} increase with temperature (Figure 4). The increase of A_{nrad} can be simply explained by the increasing probability of multiphonon relaxation with temperature. Indeed, above T_{cross} , the number of O-H(D) oscillators coordinated to Eu^{3+} increases, accounting for the higher slope of A_{nrad} as a function of temperature above T_{cross} (see Figure 4(b)). Note that the highly symmetrical structure of $[\text{Eu}(\text{H}_2\text{O})_8]^{3+}$ (see Figure 6) seems to predominate below T_{cross} .²⁷ Consequently, the emission from the ${}^5\text{D}_0$ energy level at temperatures below T_{cross} (mostly

due to 8-fold coordinated sites) is mainly ascribed to the MD radiative transition to the 7F_1 terminal level.⁴² This clearly results in low values for I_{tot}/I_{MD} and A_{rad} below T_{cross} , as found in the experimental results included in Figure 2 and 4(a) respectively. On the other hand, the progressive intrusion of a ninth water ligand above T_{cross} is likely to distort this geometry, and therefore generate a less symmetric Eu^{3+} complex (see Figure 6). According to the Judd-Olfelt theory, this would be reflected in higher values of forced ED transition rates for the 9-fold coordinated complexes, leading to an increase of I_{tot}/I_{MD} and the subsequent decrease of τ_{rad} for the 5D_0 excited state (see Figure 2). In fact, when the Eu^{3+} environment is more asymmetric, A_{rad} is expected to increase for ED forced transitions due to a larger admixing of the $4f$ orbitals with the excited $5d$ orbitals.²⁰ Moreover, the temperature induced increase of A_{rad} below and above T_{cross} can be somehow explained as a result of an increasing asymmetry. In fact, a significant increase of the asymmetry of water molecules structure with temperature has been previously shown by means of X-ray and Raman techniques.⁴³ We therefore propose that these asymmetric distortions in the Eu^{3+} local environment (affecting to both 8- and 9-fold coordinated complexes) account for the increase in A_{rad} with temperature (see Figure 4a).

At this point, it is important to note that the T_{cross} values here reported are within the T_{cross} range reported in the literature (from 20 to 50 °C). It is an interesting question why there is such a broad range of reported values for T_{cross} in the literature. We here state that this spreading in T_{cross} is very likely due to the different pH values of the aqueous solutions. To support this statement we have taken different data previously reported and investigated how the pH affects T_{cross} .^{7, 13, 44-50} **Figure 7** shows how T_{cross} changes with different pH values at 20°C for different aqueous solutions. In some cases, the pH was simply measured as a function of temperature for samples with different initial pH (the pH value at 20°C). pH values as a function of temperature present a bilinear behavior, the T_{cross} value being dependent on the pH value at 20 °C.⁴⁴⁻⁵⁰ In other cases, we used data corresponding to aqueous solutions (with a given initial pH at 20°C) that displayed the bilinear behavior on different physical properties, or aqueous dispersions of optically active nanoparticles that displayed temperature induced changes as a result of the water structural crossover.^{7, 13} Within data dispersion, a clear trend is found revealing that T_{cross} increases with pH and seems to saturate for pH values higher than 9. Nevertheless, the results given in Figure 7 reveal that pH plays an important role in the water structural crossover. Indeed, the T_{cross} value obtained for the Eu^{3+} ions in the aqueous solution investigated in this work falls nicely within the general trend.

Conclusions

In summary, in this work we provide experimental evidence of the fundamental role that the water structural crossover plays in the temperature dependence of the optical spectroscopy of diluted solutions of Eu^{3+} aqueous complexes. It is here confirmed that two coordination

compounds coexist in equilibrium, $[\text{Eu}(\text{H}(\text{D})_2\text{O})_8]^{3+}$ and $[\text{Eu}(\text{H}(\text{D})_2\text{O})_9]^{3+}$, giving rise to two non-equivalent species whose relative population depends on the structure of water molecules clusters. Thus, the water structural crossover leads to the appearance of a bilinear behavior in the temperature dependence of a variety of Eu^{3+} spectroscopic properties. This bilinear behavior is explained in terms of a temperature induced redistribution between the $[\text{Eu}(\text{H}(\text{D})_2\text{O})_8]^{3+}$ and $[\text{Eu}(\text{H}(\text{D})_2\text{O})_9]^{3+}$ coexisting complexes. At temperatures below crossover temperature, the 8-fold coordinated complex is predominant, while at temperatures above crossover temperature the 9-fold coordinated complex considerably increases its concentration. This behavior is interpreted as due to the increased concentration of “free” water molecules above the crossover temperature. The effect of this anomaly in the temperature dependence of spectroscopic properties has been traditionally ignored and points out the need of revisiting the previous interpretation of the physics behind the thermal quenching of luminescent aqueous dispersions. Finally, from an applied point of view, the results reported herein will have important implications on the temperature dependence of numerous properties of aqueous solutions, which are of great importance in biochemistry.

Acknowledgements

Work partially supported by the Ministerio de Economía y Competitividad de España (MAT2016-75362-C3-1-R), by COST Action CM1403, by Instituto de Salud Carlos III (PI16/00812), by Comunidad Autónoma de Madrid (B2017/BMD-3867RENIM-CM), by the European Commission (NanoTBTech), and “cofinanciado con Fondos Estructurales de la Union Europea”. L.L.-P. thanks Universidad Autónoma de Madrid for the “Formación de Personal Investigador (FPI-UAM)” program. E. M. thanks CONACyT for the Postdoctoral Fellowship. M. B. thanks Dipartimento di Biotecnologie, Univ. Verona, for financial support.

References

1. Chen, H.; Khemtong, C.; Yang, X.; Chang, X.; Gao, J., Nanonization Strategies for Poorly Water-Soluble Drugs. *Drug discovery today* **2011**, *16*, 354-360.
2. Fillol, J. L.; Codolà, Z.; Garcia-Bosch, I.; Gómez, L.; Pla, J. J.; Costas, M., Efficient Water Oxidation Catalysts Based on Readily Available Iron Coordination Complexes. *Nature chemistry* **2011**, *3*, 807-813.
3. Bulone, D.; San Biagio, P.; Palma-Vittorelli, M.; Palma, M.; Columbo, M. F.; Rau, D. C.; Parsegian, V. A., The Role of Water in Hemoglobin Function and Stability. *Science* **1993**, *259*, 1335-1337.
4. Russo, J.; Tanaka, H., Understanding Water's Anomalies with Locally Favored Structures. *arXiv preprint arXiv:1308.4231* **2013**.
5. Gallo, P.; Amann-Winkel, K.; Angell, C. A.; Anisimov, M. A.; Caupin, F. d. r.; Chakravarty, C.; Lascaris, E.; Loerting, T.; Panagiotopoulos, A. Z.; Russo, J., Water: A Tale of Two Liquids. *Chemical reviews* **2016**, *116*, 7463-7500.

6. del Valle, J. C.; Camarillo, E.; Martinez Maestro, L.; Gonzalo, J. A.; Aragón, C.; Marqués, M.; Jaque, D.; Lifante, G.; Solé, J. G.; Santacruz-Gómez, K., Dielectric Anomalous Response of Water at 60° C. *Philos. Mag.* **2015**, *95*, 683-690.
7. Labrador-Páez, L., et al., Unveiling Molecular Changes in Water by Small Luminescent Nanoparticles. *Small* **2017**, *13*, 1700968.
8. Maestro, L.; Marqués, M.; Camarillo, E.; Jaque, D.; Solé, J. G.; Gonzalo, J.; Jaque, F.; Valle, J. C. D.; Mallamace, F.; Stanley, H., On the Existence of Two States in Liquid Water: Impact on Biological and Nanoscopic Systems. *International Journal of Nanotechnology* **2016**, *13*, 667-677.
9. Catalán, J.; Gonzalo, J. A., Liquid Water Changes Its Structure at 43 °C. *Chem. Phys. Lett.* **2017**, *679*, 86-89.
10. Nilsson, A.; Pettersson, L. G., The Structural Origin of Anomalous Properties of Liquid Water. *Nat. Commun.* **2015**, *6*.
11. Mallamace, F.; Corsaro, C.; Mallamace, D.; Vasi, S.; Vasi, C.; Stanley, H. E., Thermodynamic Properties of Bulk and Confined Water. *The Journal of chemical physics* **2014**, *141*, 18C504.
12. Gregory, J.; Clary, D.; Liu, K.; Brown, M.; Saykally, R., The Water Dipole Moment in Water Clusters. *Science* **1997**, *275*, 814-817.
13. Labrador-Páez, L.; Pedroni, M.; Smits, K.; Speghini, A.; Jaque, F.; García-Solé, J.; Jaque, D.; Haro-González, P., Core-Shell Engineering to Enhance the Spectral Stability of Heterogeneous Luminescent Nanofluids. *Particle & Particle Systems Characterization* **2017**.
14. Parker, D., Excitement in F Block: Structure, Dynamics and Function of Nine-Coordinate Chiral Lanthanide Complexes in Aqueous Media. *Chem. Soc. Rev.* **2004**, *33*, 156-165.
15. Chatterjee, A.; Maslen, E.; Watson, K., The Effect of the Lanthanoid Contraction on the Nonaaqualanthanoid (Iii) Tris (Trifluoromethanesulfonates). *Acta Crystallographica Section B: Structural Science* **1988**, *44*, 381-386.
16. Chatterjee, A.; Maslen, E.; Watson, K., Electron Densities in Crystals of Nonaaqualanthanoid (Iii) Tris (Trifluoromethanesulfonates). *Acta Crystallographica Section B: Structural Science* **1988**, *44*, 386-395.
17. Tu, D.; Zheng, W.; Huang, P.; Chen, X., Europium-Activated Luminescent Nanoprobes: From Fundamentals to Bioapplications. *Coord. Chem. Rev.* **2017**.
18. Furet, E.; Costuas, K.; Rabiller, P.; Maury, O., On the Sensitivity of F Electrons to Their Chemical Environment. *J. Am. Chem. Soc.* **2008**, *130*, 2180-2183.
19. Buenzli, J.-C. G., On the Design of Highly Luminescent Lanthanide Complexes. *Coord. Chem. Rev.* **2015**, *293*, 19-47.
20. Binnemans, K., Interpretation of Europium (Iii) Spectra. *Coord. Chem. Rev.* **2015**, *295*, 1-45.
21. Peacock, R. D., The Intensities of Lanthanide F↔ F Transitions. In *Rare Earths*, Springer: 1975; pp 83-122.
22. Tanner, P. A., Some Misconceptions Concerning the Electronic Spectra of Tri-Positive Europium and Cerium. *Chem. Soc. Rev.* **2013**, *42*, 5090-5101.
23. Werts, M. H.; Jukes, R. T.; Verhoeven, J. W., The Emission Spectrum and the Radiative Lifetime of Eu 3+ in Luminescent Lanthanide Complexes. *Phys. Chem. Chem. Phys.* **2002**, *4*, 1542-1548.
24. Malmberg, C. G., Dielectric Constant of Deuterium Oxide. *Journal of Research of the National Bureau of Standards* **1958**, *60*, 609-612.
25. Chaussédent, S.; Monteil, A.; Ferrari, M.; Del Longo, L., Molecular Dynamics Study of Eu3+ in an Aqueous Solution: Luminescence Spectrum from Simulated Environments. *Philosophical Magazine B* **1998**, *77*, 681-688.

26. Allen, P.; Bucher, J.; Shuh, D.; Edelstein, N.; Craig, I., Coordination Chemistry of Trivalent Lanthanide and Actinide Ions in Dilute and Concentrated Chloride Solutions. *Inorg. Chem.* **2000**, *39*, 595-601.
27. Chaussedent, S.; Monteil, A.; Ferrari, M., Molecular Dynamics Simulation of Eu³⁺ in Aqueous Solution Comparison with Experimental Luminescence Spectra. *J. Lumin.* **1997**, *72*, 567-569.
28. Supkowski, R. M.; Horrocks, W. D., On the Determination of the Number of Water Molecules, Q, Coordinated to Europium (III) Ions in Solution from Luminescence Decay Lifetimes. *Inorg. Chim. Acta* **2002**, *340*, 44-48.
29. Horrocks Jr, W. D.; Sudnick, D. R., Lanthanide Ion Probes of Structure in Biology. Laser-Induced Luminescence Decay Constants Provide a Direct Measure of the Number of Metal-Coordinated Water Molecules. *J. Am. Chem. Soc.* **1979**, *101*, 334-340.
30. Max, J.-J.; Chapados, C., Isotope Effects in Liquid Water by Infrared Spectroscopy. III. H₂O and D₂O Spectra from 6000 to 0 cm⁻¹. *The Journal of chemical physics* **2009**, *131*, 184505.
31. Berry, M. T.; May, P. S.; Xu, H., Temperature Dependence of the Eu³⁺ 5d₀ Lifetime in Europium Tris (2, 2, 6, 6-Tetramethyl-3, 5-Heptanedionato). *The Journal of Physical Chemistry* **1996**, *100*, 9216-9222.
32. Blasse, G.; Sabbatini, N., The Quenching of Rare-Earth Ion Luminescence in Molecular and Non-Molecular Solids. *Mater. Chem. Phys.* **1987**, *16*, 237-252.
33. Jørgensen, C. K.; Brinen, J. S., Far Ultra-Violet Absorption Spectra of Cerium (III) and Europium (III) Aqua Ions. *Mol. Phys.* **1963**, *6*, 629-631.
34. Kusama, H.; Sovers, O. J.; Yoshioka, T., Line Shift Method for Phosphor Temperature Measurements. *Japanese Journal of Applied Physics* **1976**, *15*, 2349.
35. Ryba-Romanowski, W.; Gołab, S.; Pisarski, W.; Dominiak-Dzik, G.; Berkowski, M.; Pajaczkowska, A., Investigation of Eu³⁺ Sites in SrLaGa₃O₇, SrLaGaO₄ and SrLaAlO₄ Crystals. *J. Phys. Chem. Solids* **1997**, *58*, 639-645.
36. Clavaguéra, C.; Pollet, R.; Soudan, J.; Brenner, V.; Dognon, J., Molecular Dynamics Study of the Hydration of Lanthanum (III) and Europium (III) Including Many-Body Effects. *The Journal of Physical Chemistry B* **2005**, *109*, 7614-7616.
37. Chaussedent, S.; Monteil, A., Molecular Dynamics Simulation of Trivalent Europium in Aqueous Solution: A Study on the Hydration Shell Structure. *The Journal of chemical physics* **1996**, *105*, 6532-6537.
38. Habenschuss, A.; Spedding, F. H., The Coordination (Hydration) of Rare Earth Ions in Aqueous Chloride Solutions from X-Ray Diffraction. III. SmCl₃, EuCl₃, and Series Behavior. *The Journal of Chemical Physics* **1980**, *73*, 442-450.
39. Ciupka, J.; Cao-Dolg, X.; Wiebke, J.; Dolg, M., Computational Study of Lanthanide (III) Hydration. *Phys. Chem. Chem. Phys.* **2010**, *12*, 13215-13223.
40. Petit, L.; Borel, A.; Daul, C.; Maldivi, P.; Adamo, C., A Theoretical Characterization of Covalency in Rare Earth Complexes through Their Absorption Electronic Properties: F–F Transitions. *Inorg. Chem.* **2006**, *45*, 7382-7388.
41. Tanner, P. A.; Yeung, Y. Y.; Ning, L., What Factors Affect the 5d₀ Energy of Eu³⁺? An Investigation of Nephelauxetic Effects. *The Journal of Physical Chemistry A* **2013**, *117*, 2771-2781.
42. Blasse, G., Luminescence from the Eu³⁺ Ion in D_{4d} Symmetry. *Inorg. Chim. Acta* **1988**, *142*, 153-154.
43. Kühne, T. D.; Khaliullin, R. Z., Electronic Signature of the Instantaneous Asymmetry in the First Coordination Shell of Liquid Water. *Nat. Commun.* **2013**, *4*, 1450.

44. Buck, R.; Rondinini, S.; Covington, A.; Baucke, F.; Brett, C.; Camoes, M.; Milton, M.; Mussini, T.; Naumann, R.; Pratt, K., Measurement of Ph. Definition, Standards, and Procedures (Iupac Recommendations 2002). *Pure Appl. Chem.* **2002**, *74*, 2169-2200.
45. Covington, A.; Bates, R.; Durst, R., Definition of Ph Scales, Standard Reference Values, Measurement of Ph and Related Terminology (Recommendations 1984). *Pure Appl. Chem.* **1985**, *57*, 531-542.
46. Hunt, R. C., Conductivity and Ph Measurements in High Purity Water. *Ultrapure Water* **1986**, *3*, 39-46.
47. G. McMillan, R. M., and Teresa Wang Opportunities for Smart Wireless Ph and Conductivity Measurements Data. *InyTech Magazine*.
48. Barron, J. J., Ashton, C., & Geary, L., The Effects of Temperature on Ph Measurement. **2006**.
49. Gray, D. M.; Santini, E. P. In *Cycle Chemistry Ph Measurement*, Proceedings of Electric Utility Chemistry Workshop, Champaign, Illinois, May 1998, 1998.
50. Dotro, P.; Nardi, M.; Rodríguez, D.; Rodríguez, V., Estudio De La Evolución Del Ph En Función De La Temperatura, Club De Ciencias" Leonardo Da Vinci" Departamento De Investigación Y Desarrollo, Emet N4, De XVIII, " Hipólito Yrigoyen", Ciudad De Buenos Aires, Argentina.[Documento En Línea]. 1997.

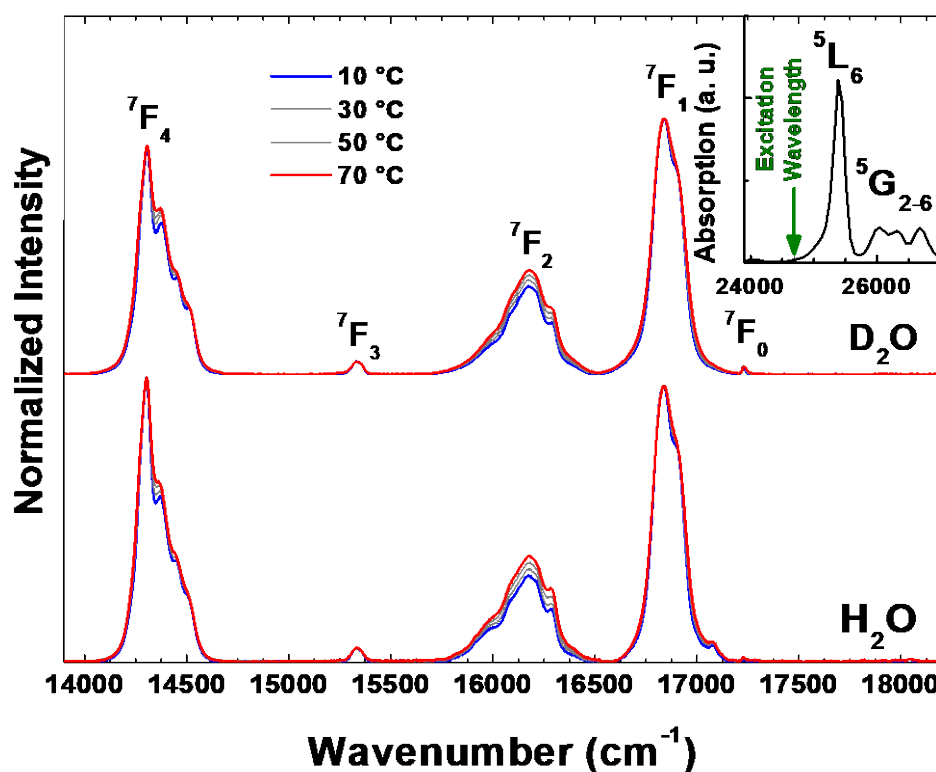


Figure 1. Emission spectra of the Eu^{3+} in D_2O (0.1 M) (top) and Eu^{3+} in H_2O (0.1 M; pH 5.5) (bottom) solutions at diverse temperatures under excitation at 405 nm (laser power 50 mW). These spectra have been normalized to the ${}^5D_0 \rightarrow {}^7F_1$ emitted intensity. Inset: absorption

spectrum of Eu^{3+} in D_2O ; the arrow indicates the excitation wavelength. Spectra have been corrected by the spectral response of the detector.

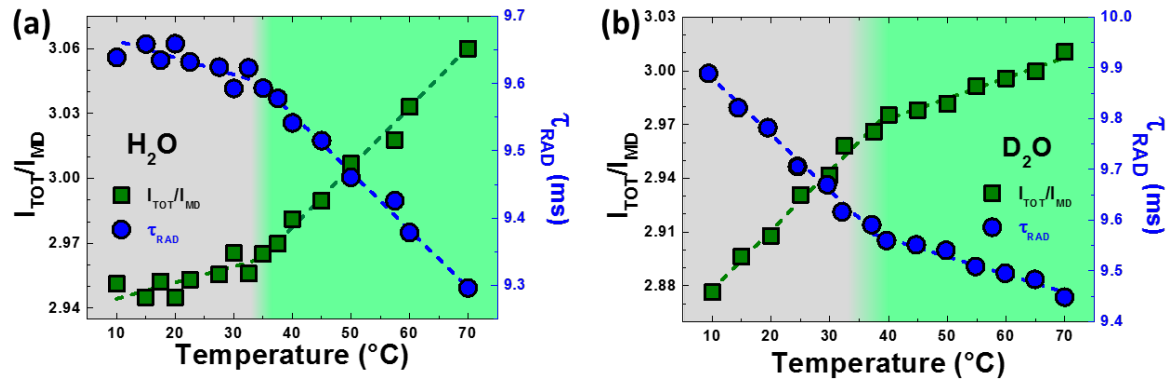


Figure 2. Temperature dependence of the total emitted intensity from the $^5\text{D}_0$ level relative to the MD $^5\text{D}_0 \rightarrow ^7\text{F}_1$ transition (squares) and of radiative lifetime of this energy level (calculated from $I_{\text{TOT}}/I_{\text{MD}}$ data using Equation (1)) (circles) for (a) the Eu^{3+} ions in H_2O and (b) the Eu^{3+} ions in D_2O solutions. Colored backgrounds delimit the temperatures below and above T_{cross} . Dashed lines are guides to the eye.

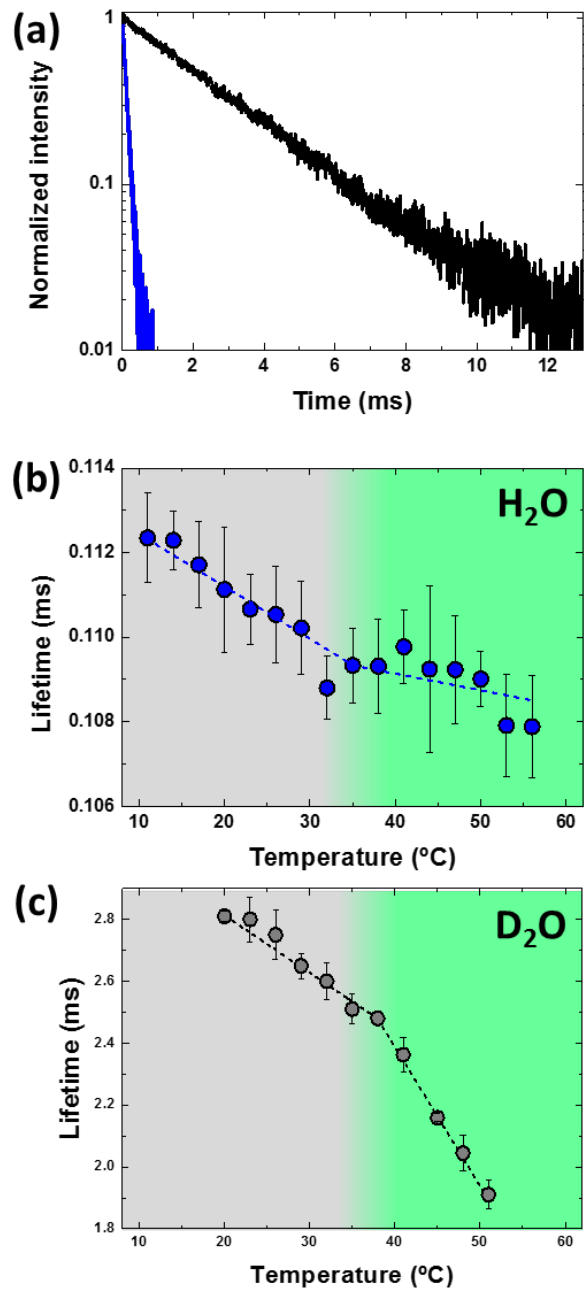


Figure 3. (a) Intensity decay curves obtained for the Eu^{3+} in H_2O and Eu^{3+} in D_2O solutions from the $^5\text{D}_0$ energy level, at 20 °C. Lifetime of the $^5\text{D}_0$ energy level of Eu^{3+} (b) in H_2O solution and in (c) D_2O solution as a function of temperature (excitation wavelength: 521 nm). Colored backgrounds delimit the temperatures below and above T_{cross} . Dashed lines are guides to the eye.

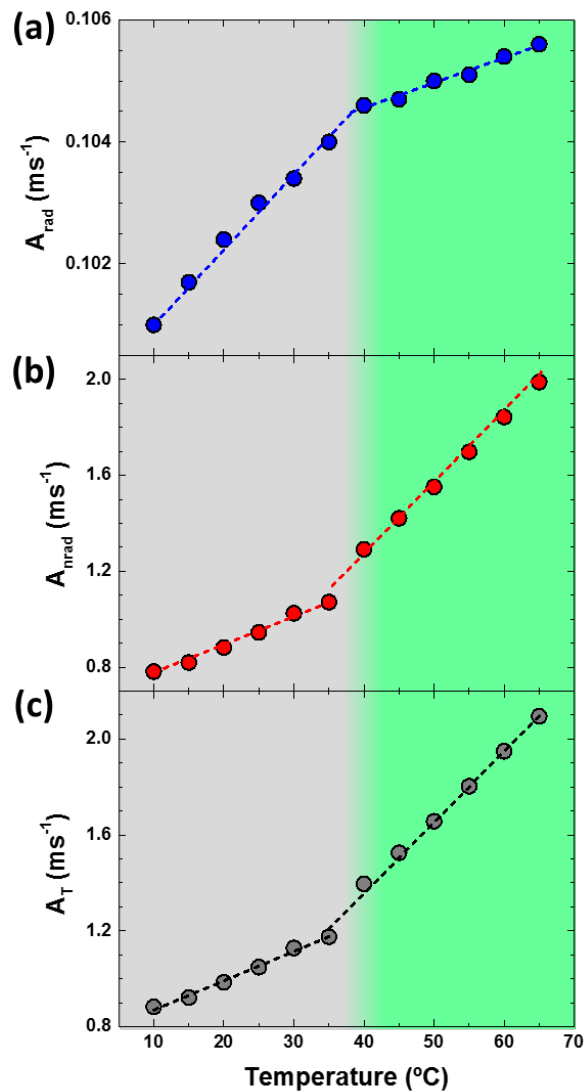


Figure 4. Temperature dependence of (a) the radiative, (b) non-radiative, and (c) total de-excitation rates estimated for Eu^{3+} in D_2O solution. Colored backgrounds delimit the temperatures below and above T_{cross} . Dashed lines are a guide to the eye.

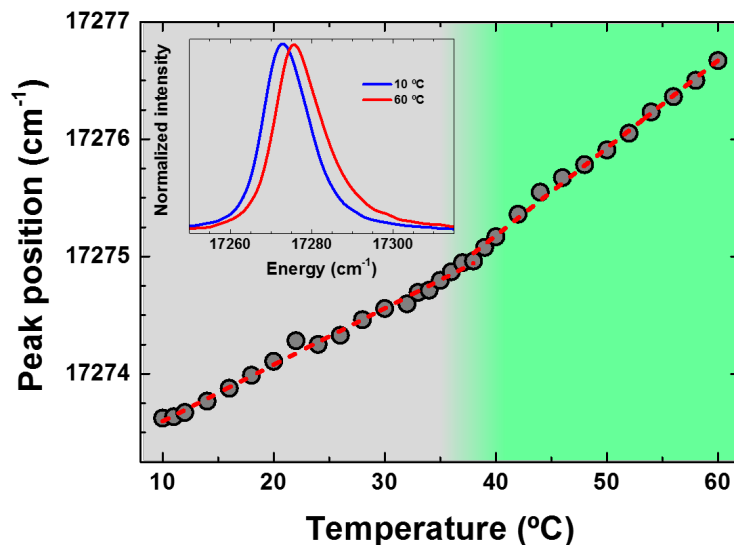


Figure 5. Peak position of ${}^5D_0 \rightarrow {}^7F_0$ emission band of Eu^{3+} in D_2O solution as a function of temperature (excitation wavelength: 405 nm). Colored backgrounds delimit the temperatures below and above T_{cross} . Dashed lines are guides to the eye. Inset: Emission spectra of this emission band at diverse temperatures.

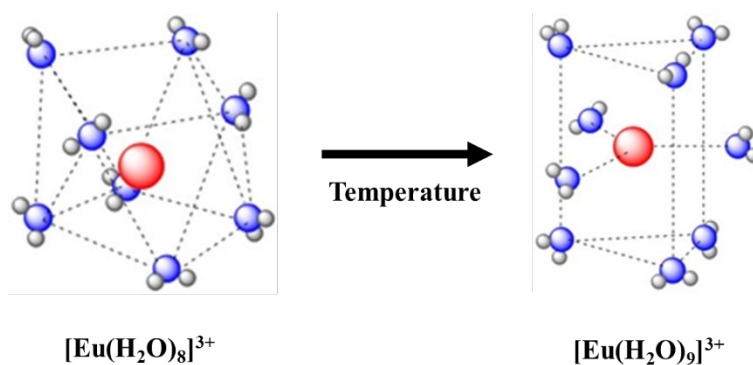


Figure 6. Schematic representations of the two Eu local environments ($[\text{Eu}(\text{H}_2\text{O})_8]^{3+}$ and $[\text{Eu}(\text{H}_2\text{O})_9]^{3+}$), where Eu^{3+} ion is schematized as a red sphere and the coordinated water molecules as blue (O^{2-}) and grey (H^+) spheres.

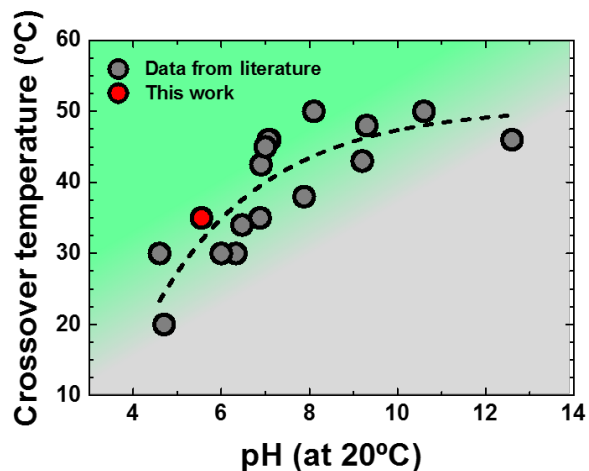


Figure 7. T_{cross} obtained from different aqueous solutions of different pH at 20 °C and from other experimental works on the water structural crossover as a function of the pH at 20 °C (gray dots). Data taken from References.^{4, 7, 27} T_{cross} spectroscopically measured in this work for the Eu^{3+} in H_2O solution (red dot). The dashed line is a guide for the eye.

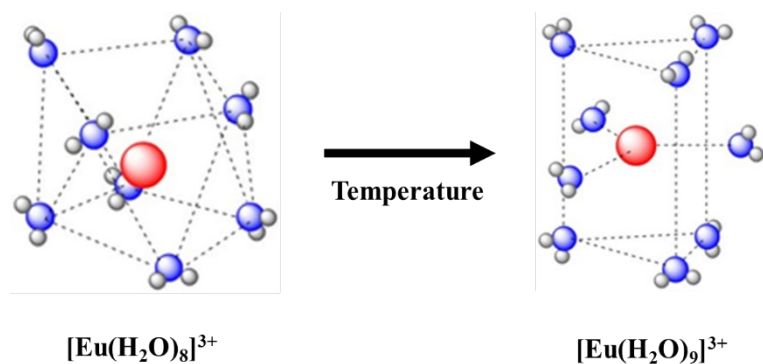


TABLE OF CONTENTS GRAPHIC